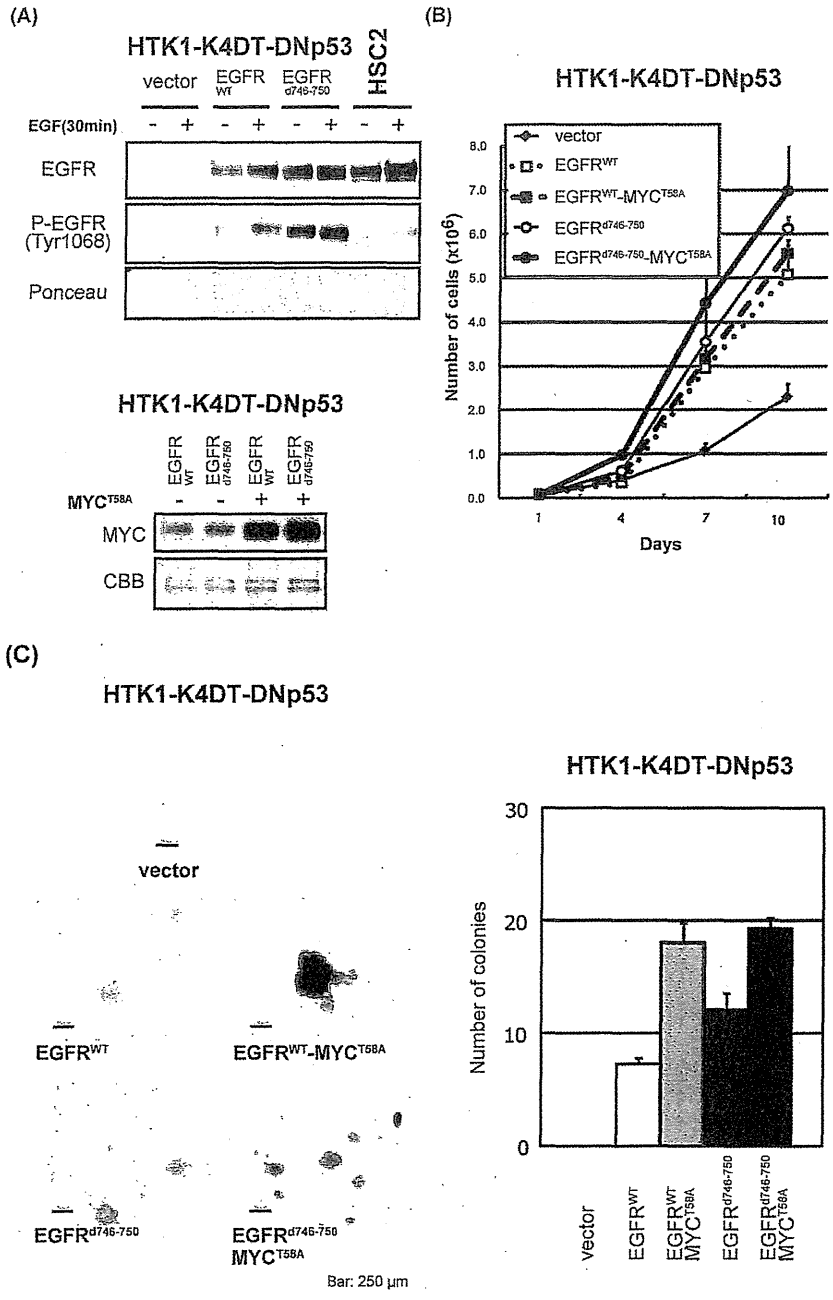

Figure 3. Anchorage-dependent and -independent growth of HTK1-K4DT-DNp53-EGFR^{WT} (or EGFR$^{d746-750}$)-MYC^{T58A} cells. (**A**) HTK1-K4DT-DNp53 cells were serially infected with retroviruses expressing EGFR^{WT}, EGFR$^{d746-750}$, MYC^{T58A} or empty vectors (-). After selection, cells were harvested and subjected to SDS-PAGE. Western blots show expression of transgenes. EGFR$^{d746-750}$; constitutively active mutant of EGFR. Cells were first starved in medium without bovine pituitary extract and EGF for 72 hours and some of them were stimulated with EGF for 30 min before harvesting as indicated. HSC2; human OSCC cell line with EGFR amplification. (**B**) Growth curves of HTK1-K4DT-DNp53 cells expressing different transgenes as described in (A). Cells were grown as described in Fig 2(B). (**C**) Anchorage-independent growth of HTK1-K4DT-DNp53 cells expressing different transgenes performed as for Fig. 2(C). Scale bars, 250 μm.

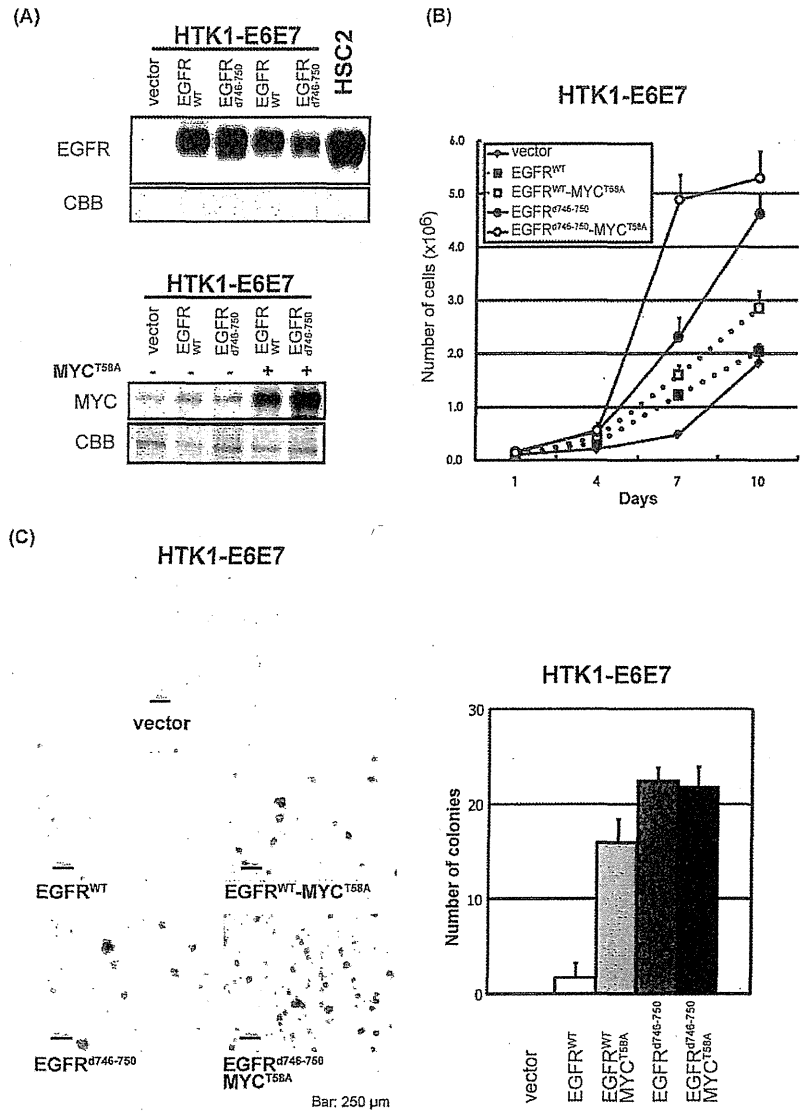

Figure 4. Anchorage-dependent and -independent growth of HTK1-E6E7-EGFR^{WT} (or EGFR$^{d746-750}$)-MYC^{T58A} cells. (**A**) HTK1-E6E7 cells were serially infected with retroviruses expressing EGFR^{WT}, EGFR$^{d746-750}$, MYC^{T58A} or empty vectors (-). After selection, cells were harvested and subjected to SDS-PAGE. Western blots show expression of transgenes. HSC2; human OSCC cell line with EGFR amplification. (**B**) Growth curves of HTK1-E6E7 cells expressing different transgenes as described in (A). Cells were grown as described in Fig 2(B). (**C**) Anchorage-independent growth of HTK1-K4DT-E6E7 cells expressing different transgenes performed as for Fig. 2(C). Scale bars, 250 μm.

4B), and showed increased anchorage-independent growth regardless of the exogenous expression of MYC^{T58A}, though those expressing EGFR^{WT} showed poor anchorage-independent growth without MYC^{T58A} (**Figure 4C**). In tumorigenic assay, HTK1-E6E7 cells expressing EGFR$^{d746-750}$ cells formed tumors only when MYC or MYC^{T58A} was co-expressed, whereas those expressing EGFR^{WT} did not form tumors even with addition of MYC or MYC^{T58A} (**Table 1**).

Histopathological findings for tumors derived from HTK1 cells.

Isolated xenograft tumors were examined by histopathologically (**Figure 5**). HTK1-K4DT-DNp53-HRAS^{G12V}-MYC^{T58A} and HTK1-K4DT-DNp53-EGFR$^{d746-750}$-MYC^{T58A} tumors mainly comprised poorly differentiated SCCs. On the other hand, tumors of HTK1-E6E7-HRAS^{G12V}-MYC^{T58A} and HTK1-E6E7-EGFR$^{d746-750}$-MYC^{T58A} cells were well differentiated SCCs with keratin pearls. Both HTK1-K4DT-DNp53-HRAS^{G12V}-MYC^{T58A} and HTK1-E6E7-HRAS^{G12V}-MYC^{T58A} cells were positive for keratin 14 proved to be carcinomatous in structure (**Figure 5**, insets).

Confirmation of the multistage nature of carcinogenesis with the HTK3T cell line.

It is possible that additional alterations (genetic and/or epigenetic) occurring during the process of introducing oncogenic genes could contribute to their tumorigenic phenotype. To address this possibility, we repeatedly transduced EGFR^{WT}, EGFR$^{d746-750}$ or HRAS^{G12V} plus MYC^{T58A} into HTK3-TE6E7 and HTK3-K4DT-DNp53 cells, another independent batch of HTKs derived from a

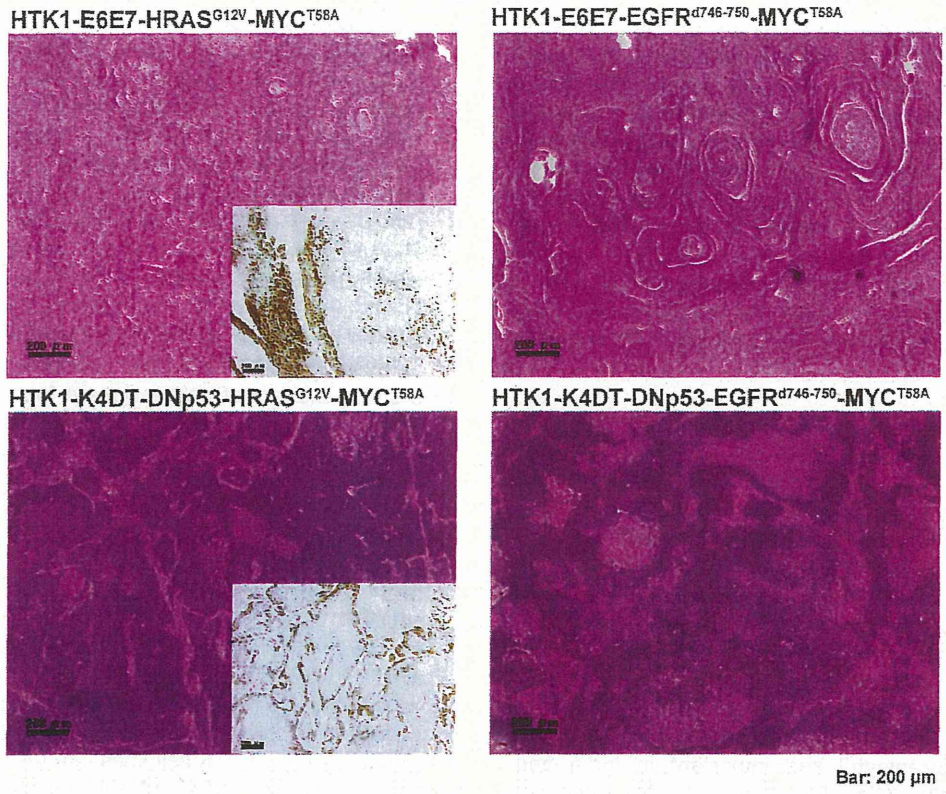

Figure 5. Histopathological findings for tumors derived from HTK1 cells. Histopathology of subcutaneous tumors of HTK1-E6E7- HRAS^{G12V}-MYC^{T58A}, HTK1-E6E7- EGFR$^{d746-750}$-MYC^{T58A}, HTK1-K4DT-DNp53-HRAS^{G12V}-MYC^{T58A} and HTK1-K4DT-DNp53-EGFR$^{d746-750}$-MYC^{T58A} cells. The insets show immunohistochemical staining of keratin 14. Scale bars, 200 μm.

different patient. All these cells reproducibly developed subcutaneous tumors in nude mice, whereas those transduced with HRAS^{G12V} alone without MYC^{T58A} and carrying empty vectors failed to form tumors (**Table 1**). The histological appearance of HTK3-K4DT-DNp53-HRAS^{G12V}-MYC^{T58A} and HTK1-TE6E7-HRAS^{G12V}-MYC^{T58A} tumors was similar to that of corresponding tumors with HTK1-K4DT and HTK1-E6E7 (data not shown). These results indicate that the combination of multiple genetic elements we applied can reproducibly fully transform HTK cells.

Discussion

Our goal is to develop an appropriate in vitro model for recapitulating development and progression of both HPV-positive and -negative human OSCCs. OSCCs are thought to arise from basal layer epithelial cells of oral mucosa, which regenerates stratified epithelium through terminal differentiation of keratinocytes. The fact that human tongue keratinocytes (HTKs) were here obtained from two patients without smoking histories or cancer, allowed us to explore inter-individual variation in the tumor formation process. In this report, we document establishment of an in vitro model system for HPV16-positive and -negative multistep carcinogenesis using normal HTKs.

As also shown earlier, overexpression of HPV16 E6 and E7 themselves could immortalize HTKs but did not support anchorage-independent growth. We next tried to immortalize HTKs without viral oncogenes to establish an in vitro model system for HPV-negative multistep carcinogenesis. By CDK4 and cyclin D1 transduction in combination with TERT, we here established novel HTK cell lines, termed HTK1-K4DT and HTK3-K4DT. The pRB pathway is frequently disrupted in OSCCs by p16^{INK4a} inactivation

and/or abnormal expression of CDK4/cyclinD1 [18, 20, 36, 37]. OSCCs, like many other carcinomas, maintain telomere length with telomerase activation [21, 22]. Immortality is one of the important characteristics of malignancy and ectopic expression of these genes thus could mimic the events that occur during development of OSCCs. Alterations of p53 have been detected in approximately 50% of OSCCs [23, 36-39] and some authors suggest that p53 alterations might represent an early step in the oral carcinogenesis, especially for HPV-negative OSCCs.

OSCCs often overexpress the epidermal growth factor receptor (EGFR) and some of its active variants or harbor activating mutations in the RAS oncogene with a rate ranging from 3% to 5% in Western countries and up to 50% in India and Southeast Asia. Importantly, EGFR mutations and KRAS mutations are mutually exclusively observed in non-small cell lung carcinomas[40]. A similar tendency has also been observed in a smaller number of OSCCs [19]. Recently, complications of chewing betel quid in oral cancer development have been found clinically meaningful and important in India and Southeast Asia. For example, EGFR amplification or a high frequency of mutations in codons 12 and 61 of the HRAS were reported to be associated with heavy betel quid users [16, 35, 37, 41]. EGFR, a key cancer-driving gene during OSCC development, belongs to the type I receptor tyrosine kinase (ERBB) subfamily, and appears more important than other ERBB members for oral cancer development [19]. In addition to gene amplification, activating mutation of genes in kinase signaling pathways is another common genetic event during cancer development. EGFR and its downstream effectors have diverse cellular functions, impacting on cell proliferation, differentiation, motility, survival, and tissue development [42]. The RAS-RAF-MAPK cascade is particularly active when cancer cells overexpress EGFR [43]. Schulze and colleagues have further shown that the majority of RAS-RAF-MAPK-induced changes in gene expression are dependent on the status of EGFR [44], highlighting the critical roles of the signal networking among different oncogenes in cancers [45]. In addition, Raimondi et al have shown that, in spite of ras being likely activated in many K14-expressing squamous epithelia in their animal system, those animals develop benign tumors only in the oral mucosa. This suggests that oral epithelial cells might be particularly sensitive to RAS-induced aberrant cell proliferation. Here, transduction of oncogenic HRAS or wild type EGFR or mutant EGFR ($EGFR^{d746-750}$) into HTK-E6E7 and HTK-K4DT-DNp53 cells resulted in enhanced anchorage-independent growth but no tumor forming ability, except when oncogenic HRAS was transduced into HTK1-E6E7. Therefore we tried to define essential genetic alterations that cooperate with $HRAS^{G12V}$ or wild type EGFR or $EGFR^{d746-750}$ to induce a fully transformed phenotype. Amplification and/or overexpression of the MYC gene, an oncogene but also a strong inducer of apoptosis, are found in 26-40% of all oral cancers [15, 20]. Furthermore, amplification of MYC is a common finding in advanced stages, which may suggest a critical role in progression. In this study, transduction of wild-type or a mutant MYC strongly enhanced anchorage-independent growth of HTK-E6E7 and HTK-K4DT-DNp53 cells expressing $HRAS^{G12V}$, $EGFR^{WT}$, or $EGFR^{d746-750}$, and resulted in tumor formation, except when MYC or MYC^{T58A} was transduced into HTK-E6E7-$EGFR^{WT}$ cells (**Table 1**). In addition, we have focused on development of an orthotopic model of OSCC through injecting HTK cell lines into the tongues of nude mice. HTK1-K4DT-DNp53-$HRAS^{G12V}$-MYC^{T58A} and HTK1-K4DT-DNp53-$EGFR^{WT}$-MYC^{T58A} cells formed orthotopic tumors (**Figure 6A**) and showed SCC-like features histopathologically (**Figure 6B**). Furthermore, one out of the four tumors yielded regional metastases in 2-3 weeks (data not shown). Further investigation with the orthotopic model should be useful to identify genes and other factors involving in regional metastases.

Human cancer cell lines, even though they are derived from well-differentiated carcinomas, rarely mimic the original histology when inoculated into mice. In our study, HTK1-K4DT-DNp53 cells expressing $HRAS^{G12V}$ or $EGFR^{d746-750}$ and MYC (HPV-negative model) formed tumors faster than HTK1-E6E7 cells expressing the same additional oncogenes (HPV-positive model), and HTK1-E6E7 cells expressing $EGFR^{WT}$ and MYC or MYC^{T58A} failed to form tumors unlike the corresponding HTK1-K4DT-DNp53 cells (**Table 1**). In addition, isolated subcutaneously xenograft tumors of HTK1-E6E7 cells expressing either $HRAS^{G12V}$ plus MYC^{T58A} or $EGFR^{d746-750}$ -MYC^{T58A} (HPV-positive model) showed histological features of well-differentiated SCCs, but the corresponding

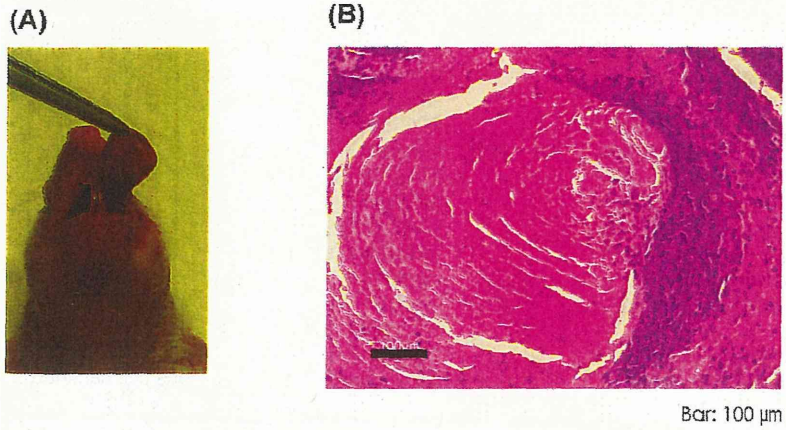

Figure 6. Orthotopic xenografts of HTK1-K4DT-DNp53-HRAS^{G12V}-MYC^{T58A} cells. (**A**) A representative tumor at day 63 after 1×10^5 cells were transplanted into the tongue of mice. (**B**) HE staining of the tumor showed SCC-like features histopathologically. Scale bar, 100 μm.

HTK1-K4DT-DNp53 cells (HPV-negative model) did not (**Figure 5**). These differences of tumorigenicity and histopathology between our HPV-positive and HPV-negative models might reflect the favorable outcome associated with HPV in oropharyngeal cancer [17, 46]. Further efforts to clarify critical pathways in carcinogenesis with each histological subtype should help provide best targets for early detection and effective molecular therapies.

In summary, we newly immortalized primary HTK cells with cellular genes (CDK4, cyclin D1 and TERT) or viral oncogenes (HPV16 E6E7). With these non-tumorigenic cell lines, we have developed for the first time an in vitro culture model faithfully recapitulating the development of HPV-positive and -negative OSCCs with genetically defined elements. Our results provide evidence that either HRAS mutation or activation of EGFR in cooperation with MYC overexpression is a strong set of drivers sufficient for transformation of HTKs which have acquired inactivation of the pRB and p53 pathways and telomerase activation by either HPV16E6E7 or equivalent genetic alterations. Our experimental model should facilitate further studies to understand genesis of OSCCs and hopefully will assist in the evaluation of new therapies.

Acknowledgements

We would like to express our appreciation to Yuki Inagawa, Shin-ichi Ohno and Takako Ishiyama for their expert technical assistance. This work was supported in part by Grants-in-Aid for Cancer Research from the Ministry of Health Labor and Welfare, for Cancer Research from the Yasuda Medical Foundation to T.K., and for Scientific Research from the Ministry of Education, Culture, Sports, Science, and Technology of Japan to Y.Z., K.N., M.U., and T.K.

Conflict of interest

Authors have no conflict of interest.

Address correspondence to: Tohru Kiyono, MD, PhD, Division of Virology, National Cancer Center Research Institute, 5-1-1 Tsukiji, Chuo-ku, Tokyo 104-0045, Japan. E-mail: tkiyono@ncc.go.jp

References

[1] Choi S and Myers JN. Molecular pathogenesis of oral squamous cell carcinoma: implications for therapy. J Dent Res 2008; 87: 14-32.

[2] Pereira MC, Oliveira DT, Landman G and Kowalski LP. Histologic subtypes of oral squamous cell carcinoma: prognostic relevance. J Can Dent Assoc 2007; 73: 339-344.

[3] Sudbo J, Bryne M, Mao L, Lotan R, Reith A, Kildal W, Davidson B, Soland TM and Lippman SM. Molecular based treatment of oral cancer. Oral Oncol 2003; 39: 749-758.

[4] Campisi G, Panzarella V, Giuliani M, Lajolo C, Di Fede O, Falaschini S, Di Liberto C, Scully C and Lo Muzio L. Human papillomavirus: its identity and controversial role in oral oncogenesis, premalignant and malignant lesions (review). Int J Oncol 2007; 30: 813-823.

[5] Psyrri A and DiMaio D. Human papillomavirus in cervical and head-and-neck cancer. Nat Clin Pract Oncol 2008; 5: 24-31.

[6] Ragin CC, Modugno F and Gollin SM. The epidemiology and risk factors of head and neck cancer: a focus on human papillomavirus. J Dent Res 2007; 86: 104-114.

[7] Gillison ML, Koch WM, Capone RB, Spafford M, Westra WH, Wu L, Zahurak ML, Daniel RW, Viglione M, Symer DE, Shah KV and Sidransky

D. Evidence for a causal association between human papillomavirus and a subset of head and neck cancers. J Natl Cancer Inst 2000; 92: 709-720.

[8] Galloway DA and McDougall JK. The disruption of cell cycle checkpoints by papillomavirus oncoproteins contributes to anogenital neoplasia. Semin Cancer Biol 1996; 7: 309-315.

[9] Scheffner M, Huibregtse JM, Vierstra RD and Howley PM. The HPV-16 E6 and E6-AP complex functions as a ubiquitin-protein ligase in the ubiquitination of p53. Cell 1993; 75: 495-505.

[10] Dyson N, Howley PM, Munger K and Harlow E. The human papilloma virus-16 E7 oncoprotein is able to bind to the retinoblastoma gene product. Science 1989; 243: 934-937.

[11] Hunter KD, Parkinson EK and Harrison PR. Profiling early head and neck cancer. Nat Rev Cancer 2005; 5: 127-135.

[12] Califano J, van der Riet P, Westra W, Nawroz H, Clayman G, Piantadosi S, Corio R, Lee D, Greenberg B, Koch W and Sidransky D. Genetic progression model for head and neck cancer: implications for field cancerization. Cancer Res 1996; 56: 2488-2492.

[13] Ryott M, Wangsa D, Heselmeyer-Haddad K, Lindholm J, Elmberger G, Auer G, Lundqvist EV, Ried T and Munck-Wikland E. EGFR protein overexpression and gene copy number increases in oral tongue squamous cell carcinoma. Eur J Cancer 2009; 45: 1700-1708.

[14] Chiang WF, Liu SY, Yen CY, Lin CN, Chen YC, Lin SC and Chang KW. Association of epidermal growth factor receptor (EGFR) gene copy number amplification with neck lymph node metastasis in areca-associated oral carcinomas. Oral Oncol 2008; 44: 270-276.

[15] Vora HH, Shah NG, Trivedi TI, Goswami JV, Shukla SN and Shah PM. Expression of C-Myc mRNA in squamous cell carcinoma of the tongue. J Surg Oncol 2007; 95: 70-78.

[16] Sathyan KM, Nalinakumari KR and Kannan S. H-Ras mutation modulates the expression of major cell cycle regulatory proteins and disease prognosis in oral carcinoma. Mod Pathol 2007; 20: 1141-1148.

[17] Na, II, Kang HJ, Cho SY, Koh JS, Lee JK, Lee BC, Lee GH, Lee YS, Yoo HJ, Ryoo BY, Yang SH and Shim YS. EGFR mutations and human papillomavirus in squamous cell carcinoma of tongue and tonsil. Eur J Cancer 2007; 43: 520-526.

[18] Freier K, Joos S, Flechtenmacher C, Devens F, Benner A, Bosch FX, Lichter P and Hofele C. Tissue microarray analysis reveals site-specific prevalence of oncogene amplifications in head and neck squamous cell carcinoma. Cancer Res 2003; 63: 1179-1182.

[19] Sheu JJ, Hua CH, Wan L, Lin YJ, Lai MT, Tseng HC, Jinawath N, Tsai MH, Chang NW, Lin CF, Lin CC, Hsieh LJ, Wang TL, Shih Ie M and Tsai FJ. Functional genomic analysis identified epidermal growth factor receptor activation as the most common genetic event in oral squamous cell carcinoma. Cancer Res 2009; 69: 2568-2576.

[20] Akervall J, Bockmuhl U, Petersen I, Yang K, Carey TE and Kurnit DM. The gene ratios c-MYC:cyclin-dependent kinase (CDK)N2A and CCND1:CDKN2A correlate with poor prognosis in squamous cell carcinoma of the head and neck. Clin Cancer Res 2003; 9: 1750-1755.

[21] Freier K, Pungs S, Flechtenmacher C, Bosch FX, Lichter P, Joos S and Hofele C. Frequent high telomerase reverse transcriptase expression in primary oral squamous cell carcinoma. J Oral Pathol Med 2007; 36: 267-272.

[22] Pannone G, De Maria S, Zamparese R, Metafora S, Serpico R, Morelli F, Rubini C, Farina E, Carteni M, Staibano S, De Rosa G, Lo Muzio L and Bufo P. Prognostic value of human telomerase reverse transcriptase gene expression in oral carcinogenesis. Int J Oncol 2007; 30: 1349-1357.

[23] Karsai S, Abel U, Roesch-Ely M, Affolter A, Hofele C, Joos S, Plinkert PK and Bosch FX. Comparison of p16(INK4a) expression with p53 alterations in head and neck cancer by tissue microarray analysis. J Pathol 2007; 211: 314-322.

[24] Shaw R. The epigenetics of oral cancer. Int J Oral Maxillofac Surg 2006; 35: 101-108.

[25] Ogi K, Toyota M, Ohe-Toyota M, Tanaka N, Noguchi M, Sonoda T, Kohama G and Tokino T. Aberrant methylation of multiple genes and clinicopathological features in oral squamous cell carcinoma. Clin Cancer Res 2002; 8: 3164-3171.

[26] Hasegawa M, Nelson HH, Peters E, Ringstrom E, Posner M and Kelsey KT. Patterns of gene promoter methylation in squamous cell cancer of the head and neck. Oncogene 2002; 21: 4231-4236.

[27] Papadimitrakopoulou V, Izzo J, Lippman SM, Lee JS, Fan YH, Clayman G, Ro JY, Hittelman WN, Lotan R, Hong WK and Mao L. Frequent inactivation of p16INK4a in oral premalignant lesions. Oncogene 1997; 14: 1799-1803.

[28] Narisawa-Saito M, Yoshimatsu Y, Ohno S, Yugawa T, Egawa N, Fujita M, Hirohashi S and Kiyono T. An in vitro multistep carcinogenesis model for human cervical cancer. Cancer Res 2008; 68: 5699-5705.

[29] Sasaki R, Narisawa-Saito M, Yugawa T, Fujita M, Tashiro H, Katabuchi H and Kiyono T. Oncogenic transformation of human ovarian surface epithelial cells with defined cellular oncogenes. Carcinogenesis 2009; 30: 423-431.

[30] Takeda Y, Mori T, Imabayashi H, Kiyono T, Gojo S, Miyoshi S, Hida N, Ita M, Segawa K, Ogawa S, Sakamoto M, Nakamura S and Umezawa A. Can the life span of human marrow stromal cells be prolonged by bmi-1, E6,

E7, and/or telomerase without affecting cardiomyogenic differentiation? J Gene Med 2004; 6: 833-845.
[31] Naviaux RK, Costanzi E, Haas M and Verma IM. The pCL vector system: rapid production of helper-free, high-titer, recombinant retroviruses. J Virol 1996; 70: 5701-5705.
[32] Miyoshi H, Blomer U, Takahashi M, Gage FH and Verma IM. Development of a self-inactivating lentivirus vector. J Virol 1998; 72: 8150-8157.
[33] Haga K, Ohno S, Yugawa T, Narisawa-Saito M, Fujita M, Sakamoto M, Galloway DA and Kiyono T. Efficient immortalization of primary human cells by p16INK4a-specific short hairpin RNA or Bmi-1, combined with introduction of hTERT. Cancer Sci 2007; 98: 147-154.
[34] Yugawa T, Handa K, Narisawa-Saito M, Ohno S, Fujita M and Kiyono T. Regulation of Notch1 gene expression by p53 in epithelial cells. Mol Cell Biol 2007; 27: 3732-3742.
[35] Chang SE, Bhatia P, Johnson NW, Morgan PR, McCormick F, Young B and Hiorns L. Ras mutations in United Kingdom examples of oral malignancies are infrequent. Int J Cancer 1991; 48: 409-412.
[36] Koontongkaew S, Chareonkitkajorn L, Chanvitan A, Leelakriangsak M and Amornphimoltham P. Alterations of p53, pRb, cyclin D(1) and cdk4 in human oral and pharyngeal squamous cell carcinomas. Oral Oncol 2000; 36: 334-339.
[37] Xu J, Gimenez-Conti IB, Cunningham JE, Collet AM, Luna MA, Lanfranchi HE, Spitz MR and Conti CJ. Alterations of p53, cyclin D1, Rb, and H-ras in human oral carcinomas related to tobacco use. Cancer 1998; 83: 204-212.
[38] Wiest T, Schwarz E, Enders C, Flechtenmacher C and Bosch FX. Involvement of intact HPV16 E6/E7 gene expression in head and neck cancers with unaltered p53 status and perturbed pRb cell cycle control. Oncogene 2002; 21: 1510-1517.
[39] Chiba I, Shindoh M, Yasuda M, Yamazaki Y, Amemiya A, Sato Y, Fujinaga K, Notani K and Fukuda H. Mutations in the p53 gene and human papillomavirus infection as significant prognostic factors in squamous cell carcinomas of the oral cavity. Oncogene 1996; 12: 1663-1668.
[40] Kosaka T, Yatabe Y, Endoh H, Kuwano H, Takahashi T and Mitsudomi T. Mutations of the epidermal growth factor receptor gene in lung cancer: biological and clinical implications. Cancer Res 2004; 64: 8919-8923.
[41] Murugan AK, Hong NT, Cuc TT, Hung NC, Munirajan AK, Ikeda MA and Tsuchida N. Detection of two novel mutations and relatively high incidence of H-RAS mutations in Vietnamese oral cancer. Oral Oncol 2009; 45: e161-166.
[42] Wang K, Yamamoto H, Chin JR, Werb Z and Vu TH. Epidermal growth factor receptor-deficient mice have delayed primary endochondral ossification because of defective osteoclast recruitment. J Biol Chem 2004; 279: 53848-53856.
[43] Hynes NE and Lane HA. ERBB receptors and cancer: the complexity of targeted inhibitors. Nat Rev Cancer 2005; 5: 341-354.
[44] Schulze A, Nicke B, Warne PH, Tomlinson S and Downward J. The transcriptional response to Raf activation is almost completely dependent on Mitogen-activated Protein Kinase Kinase activity and shows a major autocrine component. Mol Biol Cell 2004; 15: 3450-3463.
[45] Roberts PJ and Der CJ. Targeting the Raf-MEK-ERK mitogen-activated protein kinase cascade for the treatment of cancer. Oncogene 2007; 26: 3291-3310.
[46] Hong AM, Dobbins TA, Lee CS, Jones D, Harnett GB, Armstrong BK, Clark JR, Milross CG, Kim J, O'Brien CJ and Rose BR. Human papillomavirus predicts outcome in oropharyngeal cancer in patients treated primarily with surgery or radiation therapy. Br J Cancer 2010; 103: 1510-1517.

Original Paper

Pathobiology

Pathobiology 2011;78:149–161
DOI: 10.1159/000324314

Received: December 13, 2010
Accepted after revision: January 13, 2011
Published online: May 26, 2011

Aberrant Expression of Disintegrin-Metalloprotease Proteins in the Formation and Progression of Uterine Cervical Cancer

Mohammed Shaker[a, b] Yuhki Yokoyama[a] Seiji Mori[a] Masahiko Tsujimoto[d]
Naomasa Kawaguchi[a] Tohru Kiyono[c] Toru Nakano[b] Nariaki Matsuura[a]

Departments of [a]Molecular Pathology and [b]Stem Cell Pathology, Graduate School of Medicine, Osaka University, Osaka, [c]Virology Division, National Cancer Center Research Institute, Tokyo, and [d]Department of Pathology, Osaka Police Hospital, Osaka, Japan

Key Words
Disintegrin · Cervix · Cervical intraepithelial neoplasia · Tissue inhibitor of metalloprotease · ADAM · ADAMTS

Abstract
Objective: Dysregulated expression of disintegrin-metalloprotease proteins [a disintegrin and metalloproteases (ADAMs) and ADAMs with thrombospondin motif (ADAMTSs)] has been reported in many types of cancers and is believed to play an important role in cancer formation and metastasis. However, little is known about the expression of ADAMs and ADAMTSs in the development of human cervical cancer. ***Methods:*** Reverse transcriptase polymerase chain reaction and immunoblotting were performed to assess the expression of several disintegrin-metalloproteases and tissue inhibitors of metalloproteinases (TIMPs) in squamous-type cervical cancer cells and oncogenically modified keratinocytes (immortalized human cervical keratinocytes transduced with human papilloma virus-16 E6/E7 proteins with or without oncogenes). Immunohistochemistry of ADAM-9, ADAM-10 and TIMP-3 was performed on 31 primary human cervical tissue specimens of preinvasive and invasive cervical carcinoma. ***Results:*** mRNA levels of ADAM-9, ADAM-10, ADAM-12, TIMP-2 and TIMP-3 were upregulated as cervical cells progressed from dysplastic to malignant lesions compared to normal cervical cells. These results were corroborated at the protein level by Western blot analysis and immunohistochemistry. ***Conclusion:*** The expression of disintegrin-metalloproteases and their endogenous regulators was dysregulated during cervical carcinogenesis. The aberrant expression of ADAMs might contribute to the pathogenesis of cervical cancer formation and progression.

Introduction

Cervical carcinoma, a malignant neoplasm of cervix uteri, is the second-most common cancer in women worldwide. Every year, more than 550,000 new cases of cervical cancer are diagnosed, and it contributes to the deaths of more than 310,000 women, the majority of which occur in the developing countries [1]. Squamous cell carcinoma is the most common histological type of cervical carcinoma, representing about 85–90% of all cases. Numerous studies have provided evidence that persistent infection with certain 'high-risk' human papilloma virus (HPV) strains is one of the initiating factors in the development of uterine cervical carcinoma [2]. The

KARGER

Fax +41 61 306 12 34
E-Mail karger@karger.ch
www.karger.com

1015–2008/11/0783–0149$38.00/0

Accessible online at:
www.karger.com/pat

Prof. Dr. Nariaki Matsuura
Department of Molecular Pathology, Graduate School of Medicine, Osaka University
1-7 Yamadaoka, Suita
Osaka 565-0871 (Japan)
Tel. +81 6 6879 2595, E-Mail matsuura@sahs.med.osaka-u.ac.jp

integration of HPV genome into the host DNA causes malignant transformation through the integration of viral E6 and E7 oncogenes into the host genome; these oncogenes deregulate the cell cycle regulators p53 and retinoblastoma proteins [2, 3]. However, most infections resolve spontaneously and pass uneventfully. Progression of low-grade squamous intraepithelial lesions (LSILs) to high-grade squamous intraepithelial lesions (HSILs) and subsequent invasion is linked to the persistence of HPV infection and to genetic and/or epigenetic alteration(s), which may act synergistically or independently [4].

A disintegrin and metalloproteases (ADAMs) are transmembrane proteins with broad tissue distribution. The structure of ADAMs is closely related to that of snake venom proteins [5]. ADAMs are multidomain proteins that comprise a prodomain, a zinc metalloprotease domain, a disintegrin domain, a cysteine-rich region, an epidermal growth factor-like region, a transmembrane domain and a cytoplasmic domain.

The ADAM with thrombospondin motif (ADAMTS) family of proteins is structurally related to ADAMs; however, they lack epidermal growth factor-like sequences and the transmembrane domains and are characterized by the presence of a variable number of thrombospondin-like motifs. Hence, they are soluble secreted proteins [6]. ADAMs play critical roles in physiological, inflammatory and pathological conditions through ectodomain shedding of cell ligands and the modulation of cell-cell and cell-matrix interactions [7–9]. ADAMs are involved in specific cellular processes including fertilization, neurogenesis and adipogenesis [10–13].

An increasing body of evidence indicates that disintegrin-metalloprotease proteins are involved in the formation and progression of a variety of cancers [14, 15] through regulation of cell adhesion, migration and invasion. ADAMTS-1 was found to be a regulator of metastasis depending on its catalytic domain and protein status [16, 17]. Taken together, these findings may suggest a pivotal role of ADAMs and ADAMTSs as a distinct group of oncogenes or tumor suppressor proteins [18]. Disintegrin-metalloprotease molecules share structural homology with the matrix metalloproteases (MMPs), a family of zinc-dependent proteases, in that they share a metalloprotease domain. However, half of ADAMs exert catalytic activities [19, 20]. Tissue inhibitors of metalloproteases (TIMPs), known to be potent physiological inhibitors of MMPs, can also selectively regulate the activities of specific ADAMs and ADAMTSs [21–23].

The molecular mechanisms underlying progression from normal epithelium through preinvasive cervical lesions to invasion are complex and poorly understood. Proteolysis, due to upregulation of proteases, is one of the hallmarks of cancer progression [24]. Members of the MMP family are implicated in the pathogenesis and progression of cervical carcinoma [25, 26]. Because of the close similarity between MMPs and the disintegrin-metalloprotease family, we speculated that ADAMs and ADAMTSs might play a role in cervical tumorigenesis.

Materials and Methods

Cell Lines

The cervical cancer cell lines of the squamous type (QG-U, SKG-IIIb and Yumoto) were kindly provided by Dr. Minoru Ueki (Osaka Medical College, Osaka, Japan) [27]. QG-U and SKG-IIIb cell lines are HPV positive, while the Yumoto cell line is HPV negative [28]. Cells were cultured in RPMI-1640 (Nissui, Tokyo, Japan) supplemented with 10% heat-inactivated fetal bovine serum (Biowest, Tokyo, Japan) and cultured at 37°C with 5% CO_2. The in vitro multistep cervical carcinogenesis model was chosen to assess the expression profile of proteases at the mRNA and protein levels during the course of cervical carcinogenesis. The model of oncogenically modified human cervical keratinocytes has been thoroughly described in previous literature [29]. Briefly, human cervical keratinocytes (HCK) were obtained from donors with informed consent. Keratinocytes were sequentially transduced with hTERT, HPV-16 E6E7 (viral oncoproteins) and/or oncogene(s) of interest such as Hras and c-Myc. Immortalized HCK transduced with HPV-16 E6E7 have similar characteristics to LSILs. HCK transduced with E6E7 and Hras oncogenes are similar to HSILs. Immortalized HCK with E6E7/Hras/c-Myc oncogenes had features of invasive cervical cancer. The latter 2 types of oncogenically modified cells were confirmed to be resistant to contact inhibition and differentiation. Cells were grown in defined keratinocyte serum-free medium (Gibco, New York, N.Y., USA) supplemented with growth supplement (Gibco) and cultured at 37°C with 5% CO_2.

RNA Extraction and Reverse Transcription Polymerase Chain Reaction

Total RNA was extracted using sepasol-RNA I (Nacalai Tesque, Kyoto, Japan). Genomic DNA contamination was eliminated by use of DNase (Promega, Madison, Wisc., USA). A volume of 5 μg of total RNA measured with a U-1800 spectrophotometer (Epson, Japan) was reverse transcribed with 5 units of reverse transcriptase (RT; Promega) and mixed with 0.5 μg of oligo (dT), 5 μl of 5× buffer, 2 μl of 2 mM deoxynucleotide triphosphate mixture and 40 units of RNasin. The resulting mixture (25 μl) was incubated at 42°C for 60 min and then at 65°C for 15 min. A thermal cycler (GeneAmp® PCR System 9700, PE Applied Biosystems) was used for the PCR reaction. In a PCR tube, 12.5 μl of Amplitaq Gold® PCR master Mix (Roche, N.J., USA), 9.5 μl of distilled water, 1 μl of each specific paired primer (Operon, Japan) and 1 μl of cDNA were mixed together. The primer sequences are given in table 1. The resultant mixture was denatured at 95°C for 5 min, followed by cycles of 30 s at 95°C, 45 s at the respective annealing temperature (table 1) and 1 min at 72°C as an extension

Table 1. The primer sequences designed for the RT-PCR analysis

Target gene		Primer sequence	Cycles n	Tm °C	Product size, bp
ADAM-9	forward	5′-GCTAGTTGGACTGGAGATTTGG-3′	30	57.7	486
	reverse	5′-TTATTACCACAGGAGGGAGCAC-3′		57.7	
ADAM-10	forward	5′-AATTCTGCTCCTCTCCTGGGC-3′	30	59.5	299
	reverse	5′-TATGTCCAGTGTAAATATGAGAGG-3′		54.4	
ADAM-12 L	forward	5′-CCAGAACAACTCGGCTCACT-3′	28	57.5	481
	reverse	5′-AGGCCTTGATCAGAAAGCAA-3′		53.4	
ADAM-12 S	forward	5′-TCAGTGCTGCTCCTGAGAGA-3′	28	57.5	449
	reverse	5′-AAGGGTTGGTGACTCTGTGG-3′		57.5	
ADAM-15	forward	5′-CAAATATAGGTGGCACTGAGGAG-3′	30	57.8	286
	reverse	5′-TAGCAGCAGTTCTCCAAAGTGTG-3′		57.8	
ADAM-17	forward	5′-ATGAGGCAGTCTCTCCTATTCCTGAC-3′	28	61.2	456
	reverse	5′-AAGTGGCTCTATGTTATATTCGGCCC-3′		59.6	
ADAMTS-1	forward	5′-ACGGCAGTGGTCTAAAGCAT-3′	30	55.4	312
	reverse	5′-AGTTCCAACATCAGCCATCC-3′		55.4	
ADAMTS-2	forward	5′-CTACGTCCAGAGCAGGGGTA-3′	30	59.5	336
	reverse	5′-GAACTCCTCCTCCTCCATCC-3′		59.5	
ADAMTS-3	forward	5′-TAGAAAGGGGAAACCCATCC-3′	30	55.4	243
	reverse	5′-CCCGTTTCATGGGCTACTAC-3′		57.5	
ADAMTS-4	forward	5′-TGCATCTGCCTGTGACTTTC-3′	30	55.4	433
	reverse	5′-GTTGGGCAGTCCTCAGTGTT-3′		57.5	
ADAMTS-5	forward	5′-GGACCTACCACGAAAGCAGA-3′	30	57.5	411
	reverse	5′-CCTCTTCCCTGTGCAGTAGC-3′		59.5	
ADAMTS-8	forward	5′-ACTGACATGGACGGGAATCT-3′	30	55.4	216
	reverse	5′-GAGTCCACCACATGGTCACA-3′		57.5	
ADAMTS-9	forward	5′-TCGCTCCACTGTTCACTGTC-3′	28	57.5	297
	reverse	5′-CCTGTTGAGGGCTCTCTCTG-3′		59.5	
ADAMTS-15	forward	5′-CTCCAAGCCCTGTCCTTACA-3′	30	57.5	337
	reverse	5′-CCAGATTGCAGGATCGGTAT-3′		55.4	
TIMP-1	forward	5′-TGGCACTCATTGCTTGTGGACG-3′	28	58	203
	reverse	5′-TCCGGAAGAAAGATGGGAGTGGGA-3′		58.8	
TIMP-2	forward	5′-TTCTGCACGGGGCTTTCTGCAT-3′	28	57	528
	reverse	5′-TGCTTTGGGGTTGCCGCTGAAT-3′		57	
TIMP-3	forward	5′-TCCTGAACCGTGTTTGTTGA-3′	28	59.5	249
	reverse	5′-CTTGACTGTGCTTGGTGGAA-3′		58.9	
β-Actin	forward	5′-CGCCGCCAGCTCACCATGGA-3′	30	59	611
	reverse	5′-CTGTAGCCGCGCTCGGTGAG-3′		59	

Tm = Melting temperature; ADAM-12 L = long isoform of ADAM-12; ADAM-12 S = short isoform of ADAM-12.

step. Using electrophoresis, the PCR products were run on 1.2% agarose gel and visualized with ethidium bromide stain.

Real-Time PCR

The mRNA expression levels of selected ADAMs, ADAMTSs and TIMPs were quantified by real-time PCR and normalized to the mRNA expression level of glyceraldehyde-3-phosphate dehydrogenase (GAPDH). Sequences of the primers used are shown in table 2. PCR reactions were run in a LightCycler 480 System (Roche) and carried out in a 96-well PCR plate format. Volumes of 17 μl of LightCycler SYBR Green I Master mix (Roche), 0.5 μM forward and reverse primer and 1 μl of cDNA template (20 μl in total) were made and mixed well. The thermal profile of real-time PCR reactions was as follows: heating at 95°C for 10 min followed by 50 cycles of 10 s of denaturation at 95°C, 20 s at the respective annealing temperature (table 2) and 10 s of amplification at 72°C. Experiments were performed in triplicate, and samples were subjected to agarose gel electrophoresis and ethidium bromide visualization to exclude nonspecific PCR. The fluorescence emitted from the SYBR green dye was read by the instrument after completion of each cycle, and the results were normalized to the mRNA expression of GAPDH.

Table 2. The primer sequences designed for the real-time RT-PCR analysis

Target gene		Primer sequence	Cycles, n	Tm, °C	Product size, bp
ADAM-9	forward	5′-TGGAACTGCAGGAATGGCA-3′	50	58	72
	reverse	5′-CCAAACACATTAATCCCGCC-3′		58	
ADAM-10	forward	5′-ACAGCCCATTCAGCAACCC-3′	50	57	67
	reverse	5′-GCGTCTCATGTGTCCCATTTG-3′		57	
ADAM-12 L	forward	5′-AGGCCAGAGCCAAGGGGCTT-3′	50	60	88
	reverse	5′-TGGGAGCCTGCCTGCCAGTT-3′		60	
ADAM-12 S	forward	5′-TACCACTCTGGCAGGCCCCA-3′	50	59	111
	reverse	5′-ACACTGGGCCCAACCCTTGC-3′		59	
ADAMTS-1	forward	5′-CGTCTCACCAAAGGACAGGT-3′	50	58	114
	reverse	5′-GAGGTGGAATCTGGGCTACA-3′		58	
TIMP-1	forward	5′-TCTGAAAAGGGCTTCCAGTCCCGT-3′	50	59	95
	reverse	5′-ATTCAGGCTATCTGGGACCGCA-3′		58	
TIMP-2	forward	5′-AATGAAACCGAAGCTTGGCGGC-3′	50	59	92
	reverse	5′-TGCTTTGGGGTTGCCGCTGAAT-3′		59	
TIMP-3	forward	5′-CTTTCTCCTCTGTGCCTGCT-3′	50	59	86
	reverse	5′-CTTGACTGTGCTTGGTGGAA-3′		59	
GAPDH	forward	5′-CAATGACCCCTTCATTGACC-3′	50	59	159
	reverse	5′-TTGATTTTGGAGGGATCTCG-3′		59	

Tm = Melting temperature; ADAM-12 L = long isoform of ADAM-12; ADAM-12 S = short isoform of ADAM-12.

Antibodies

Commercially available antibodies used were as follows: mouse antihuman ADAM-9 directed against the ectodomain (R&D), goat anti-ADAM-9 polyclonal antibody directed against the C terminus (Santa Cruz, USA), rabbit antihuman ADAM-10 polyclonal antibody directed against the C terminus (Millipore, USA), rabbit antihuman ADAM-12 directed against the cytoplasmic domain (Triple Point Biologics, Forest Grove, Oreg., USA), rabbit antihuman TIMP-2 polyclonal antibody (Chemicon, Temecula, Calif., USA), mouse antihuman TIMP-3 monoclonal antibody (Abcam, Tokyo, Japan) and mouse antihuman β-actin (Abcam).

Immunoblotting

Cell cultures were washed 3 times with phosphate-buffered saline and resuspended in lysis buffer containing 50 mM Tris-HCl (pH 8), 120 mM NaCl, 1 mM EDTA and 1% protease inhibitors (Calbiochem, USA). The cell lysates were centrifuged at 15,000 rpm for 10 min at 4°C, and the resultant supernatants were collected. Protein concentration was measured using the Bio-Rad protein assay (Hercules, Calif., USA). A total of 20 μg of protein sample was resolved using 10% SDS polyacrylamide gel electrophoresis and transferred onto methanol-pretreated polyvinylidene difluoride membranes (Millipore). Membranes were blocked with 5% nonfat milk and incubated with primary antibodies overnight at 4°C. The primary antibodies were used at the following dilutions: anti-ADAM-9, 1:500; anti-ADAM-10, 1:500; anti-ADAM-12, 1:1,000; anti-TIMP-2, 1:1,000; anti-TIMP-3, 1:1,000, and anti-β-actin, 1:3,000. The membranes were then washed 3 times in Tris-buffered saline containing 0.05% Tween and incubated for 1 h at room temperature in horseradish peroxidase-conjugated antirabbit or antimouse IgG at a dilution of 1:2,500. Chemiluminescent detection of horseradish peroxidase was achieved with Pierce Western blotting substrate (Thermo Scientific, USA) according to the manufacturer's instructions. The membranes were exposed to X-ray film, and the band densities were analyzed using NIH ImageJ software. Each value was normalized to the band density of the respective β-actin band.

Tissue Samples and Immunohistochemistry

Thirty-one formalin-fixed, paraffin-embedded cervical tissue blocks were obtained from the Department of Obstetrics and Gynecology of the Osaka Police Hospital. Histopathological diagnosis of each specimen was made independently by two pathologists. Tissue blocks were LSILs (n = 12), HSILs (n = 11) or invasive squamous cell carcinoma (n = 8). Informed consent was obtained from patients before the procedures, and the study was approved by the Osaka University review board. Tissue sections (4–5 μm) from representative paraffin blocks were deparaffinized in xylene and rehydrated in graded ethanol. The sections were subjected to heating in target retrieval buffer for 20 min. Endogenous peroxidases were blocked using 10% hydrogen peroxide for 15 min. Further blocking was carried out by incubating the sections with 5% bovine serum albumin for 30 min. The slides were then incubated with the primary antibody at 4°C in a moist chamber overnight. The primary antibodies were anti-ADAM-9 (1:50; R&D), anti-ADAM-10 (1:100; Millipore) and anti-TIMP-3 (1:100; Abcam). The slides were then incubated with specific secondary antibody at a dilution of 1:100 for 30 min at room temperature. The sections were incubated with streptavidin (Chemicon) at a dilution of 1:100 for 30 min. The sections were treated with 3,3′-diamino-

benzidine as a chromogen, and finally slides were counterstained with hematoxylin. Negative controls were included, with the omission of primary antibodies.

Evaluation of Immunoreactivity

The immunoreactivity was judged according to the distribution of staining (membranous, cytoplasmic and nuclear) and semiquantitative assessment of immunoreactivity, i.e. brown nuclear and cytoplasmic reactivity. A simplified scoring system was developed by calculating the percentage of immunoreactive cells. For each slide, nearly 3,000 cells were assessed for expression of a given antigen. The immunoreactivity was scored as negative (no reactive cells), weak (<10% reactive cells), moderate (11–50%) or strong (50–100%).

Statistical Analysis

Data from densimetric studies of multiple experiments were calculated for graphical depiction and statistical analysis. Student's t test was used to construct 95% confidence intervals for the differences in the various cell lines. ADAM expression in normal cervical tissue, LSILs, HSILs and cervical cancer was compared using analysis of variance. Statistical significance was defined by a p value of <0.05.

Results

Differential Expression of ADAM and ADAMTS mRNAs

To determine the expression of ADAMs and ADAMTSs in cervical cells, and to investigate their aberrant expression (if any) during cervical carcinogenesis, we performed conventional PCR analysis using an in vitro multistep carcinogenesis model of cervical cancer and human squamous cervical cancer cell lines.

ADAMs with an active catalytic domain, such as ADAM-9, -10, -12, -15 and -17, together with ADAMTS-1, -2, -3, -4, -5, -8, -9 and -15, were evaluated in our study. Levels of ADAM-9, -10 and -12 mRNAs were gradually upregulated in the oncogenically modified keratinocytes and in the cancer cell lines compared to the normal keratinocytes. ADAM-15 mRNA was detected only in normal keratinocytes and in the cancer cell lines (fig. 1).

Among the ADAMTSs tested, only ADAMTS-1 showed expression in carcinogenesis steps and in cancer cell lines (fig. 1). ADAMTS-3 mRNA was expressed in all the cancer cell lines, with no expression in the oncogenically modified cells. ADAMTS-2 mRNA was not detected in either of the groups. Some ADAMTSs were expressed sporadically in some cervical cancer cell lines (fig. 1).

To obtain more sensitive measurement, we performed real-time quantitative RT-PCR analysis using mRNAs from oncogenically modified cells and cervical cancer cell lines.

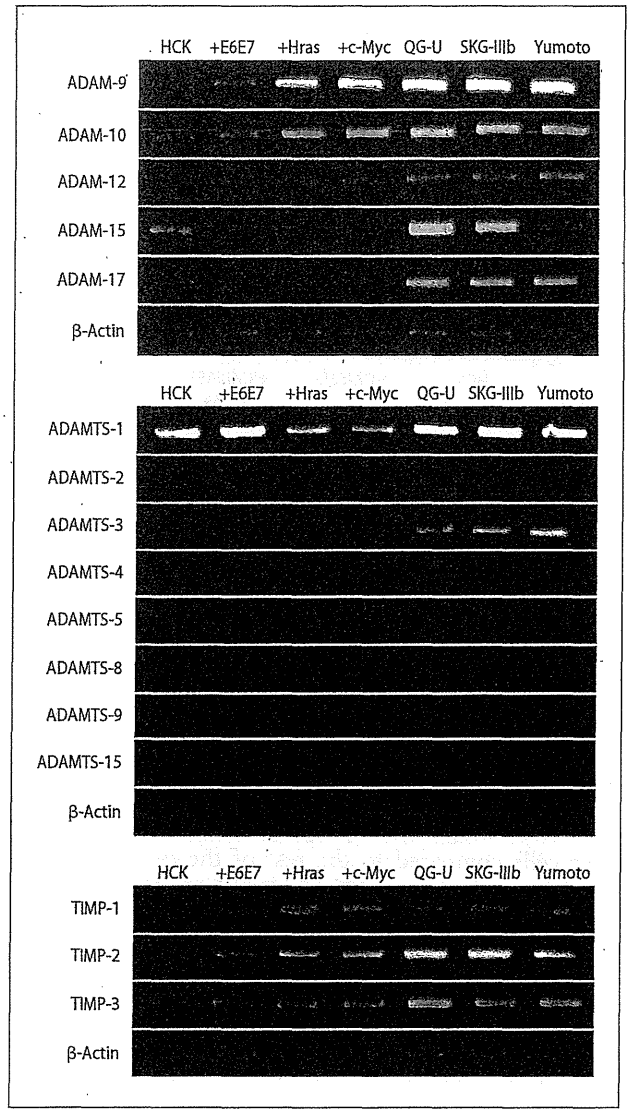

Fig. 1. RT-PCR analysis of ADAMs, ADAMTSs and TIMPs mRNA expression in normal keratinocytes (HCK = control cells), oncogenically modified keratinocytes (+E6E7 = LSILs; +Hras = HSILs; +c-Myc = invasive lesions) and squamous-type cervical cancer cell lines (QG-U, SKG-IIIb and Yumoto). The products were separated by agarose gel electrophoresis and stained with ethidium bromide.

The changes in ADAMs mRNA levels were normalized for levels of GAPDH mRNA in the same PCR. Alternative splicing of the ADAM-12 gene produces 2 isoforms, 1 long and 1 short; therefore, 2 pairs of primers were designed. A two-fold increase (a value of 2) or decrease (a value of 1) was considered target gene mRNA

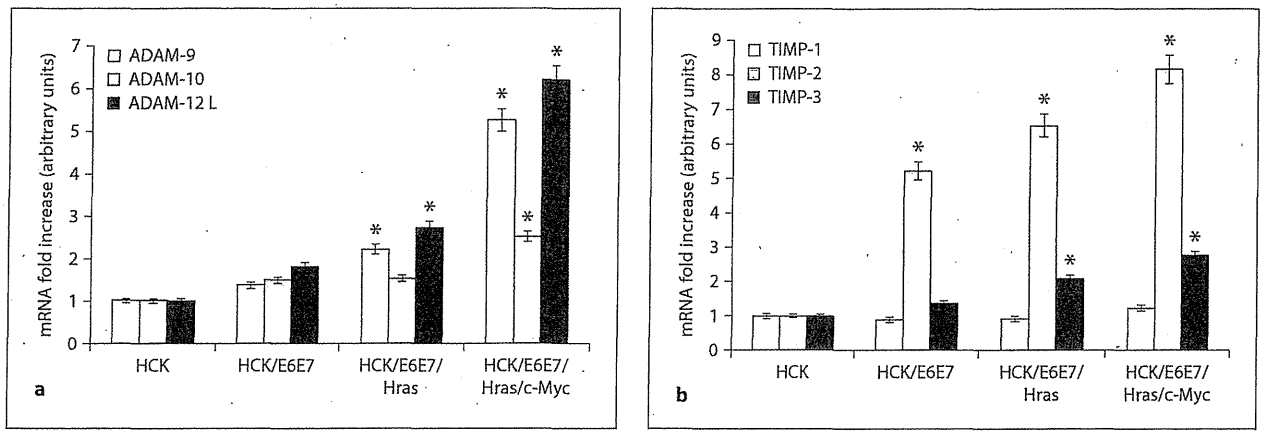

Fig. 2. Quantitative RT-PCR analysis of ADAM-9, ADAM-10 and the long form of ADAM-12 (ADAM-12 L) (**a**) and TIMP-1, -2 and -3 mRNAs (**b**) in oncogenically modified keratinocytes (HCK/E6E7 = LSILs; HCK/E6E7/Hras = HSILs; HCK/E6E7/Hras/c-Myc = invasive lesions) compared to control cells (HCK). Values for ADAMs and TIMPs in the different oncogenic stages were normalized relative to the expression levels of normal keratinocytes and normalized to the housekeeping gene (GAPDH). * $p < 0.05$.

upregulation or downregulation, respectively. The expression of ADAM-9 and the long form of ADAM-12 mRNA was significantly elevated in E6E7/Hras and E6E7/Hras/c-Myc cells compared to normal and E6E7 cells ($p < 0.05$; fig. 2a). The expression of ADAM-10 mRNA was significantly upregulated in E6E7/Hras/c-Myc cells compared to the rest of the cells ($p < 0.05$; fig. 2a). Quantitative PCR of ADAM-15, ADAM-17 and ADAMTS-1 did not show significant modulation.

Immunoblotting and Quantification of ADAMs

Immunoblotting was essential to corroborate the results obtained by quantitative RT-PCR analysis and to study the protein status. Quantitative image analysis, using β-actin as an internal housekeeping gene, was used to correct for protein loading between the control and test lanes in each experiment.

Immunoblotting of ADAM-9 protein showed 3 different bands, migrating with molecular masses of 114, 85 and 50 kDa, which represent the precursor, mature and processed forms of ADAM-9, respectively (fig. 3a, b). The ADAM-9 precursor form (114 kDa) was expressed in E6E7/Hras ± c-Myc-transduced keratinocytes and undetectable in E6E7-transduced and normal cervical keratinocytes. There was no significant difference in the frequency of expression of the ADAM-9 mature form (85 kDa) among the oncogenically modified cells. Modest upregulation of expression of the processed form (50 kDa) could be noticed as cells acquired viral E6E7 and progressed into tumorigenesis (fig. 3a). Similarly, cervical cancer cell lines (QG-U and Yumoto) showed significant upregulation of the processed form of ADAM-9 compared to normal cells ($p < 0.05$; fig. 3b).

Analysis of ADAM-10 revealed a band corresponding to a relative mass of approximately 85 kDa. ADAM-10 showed upregulation as keratinocytes acquire viral oncoproteins and genetic alteration(s) (fig. 3c). Densitometry analysis showed that the relative protein concentration was most prominent in the E6E7/Hras ± c-Myc-transduced keratinocytes compared to normal cervical keratinocytes ($p < 0.05$). Similarly, the level of ADAM-10 protein was upregulated in QG-U cancer cells compared to the normal cervical keratinocytes (fig. 3d).

Western blotting of ADAM-12 revealed a band corresponding to a molecular weight of about 84 kDa. Analysis showed that ADAM-12 was not expressed in normal cervical cells, but expression was noticed in E6E7 and E6E7/Hras ± c-Myc-transformed cells. Similarly, ADAM-12 protein was expressed in all the cervical cancer cell lines (fig. 3e, f).

Expression of TIMPs: The Physiological Inhibitors of ADAMs

mRNA levels of TIMP-1, -2 and -3 were analyzed by semiquantitative RT-PCR (fig. 1) and real-time PCR. Interestingly, quantitative RT-PCR showed that the transcript levels of TIMP-2 and TIMP-3, but not TIMP-1, were upregulated as cervical cells became carcinogenic compared with normal keratinocytes ($p < 0.05$; fig. 2b).

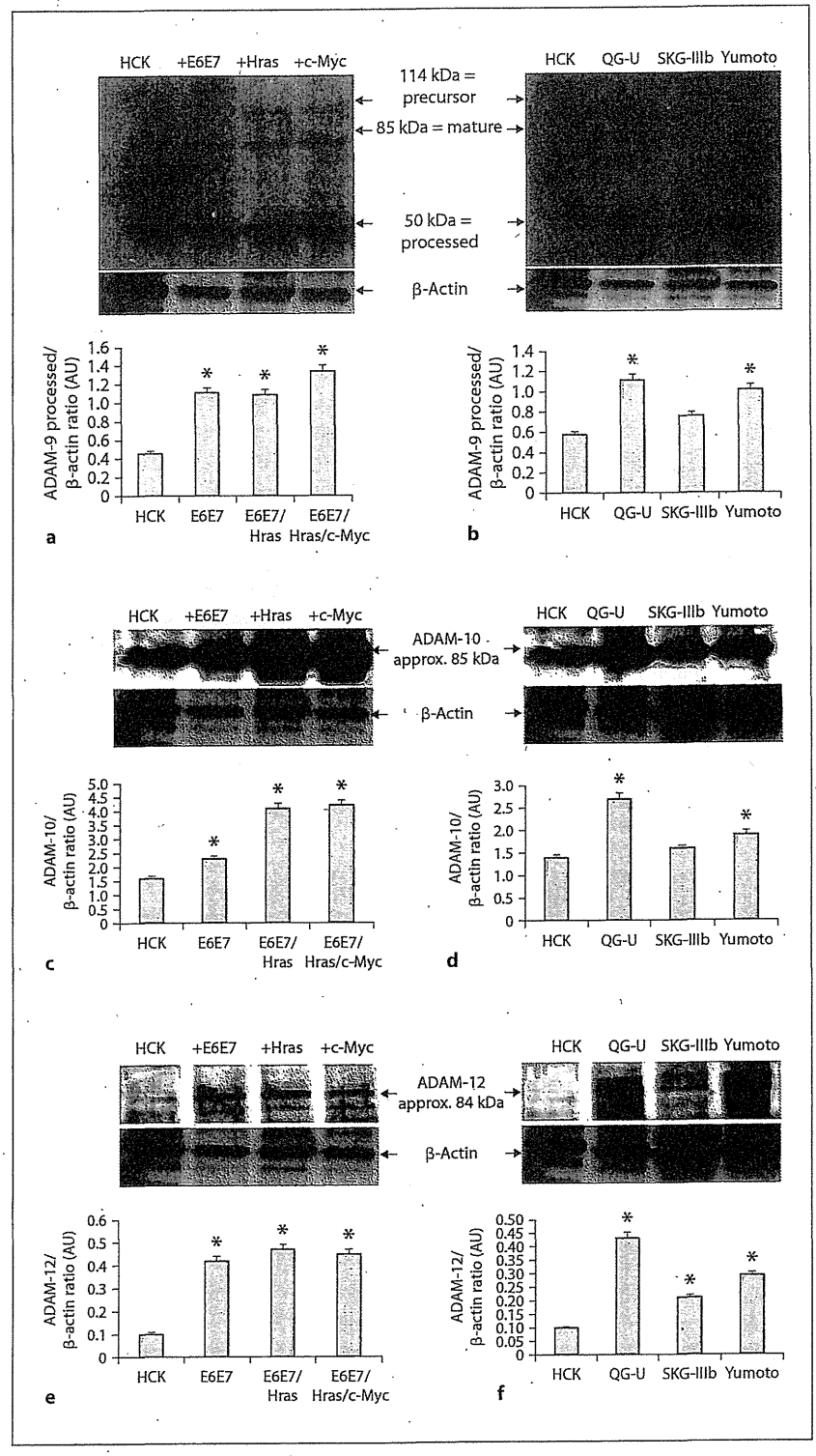

Fig. 3. Immunoblotting of ADAM-9, -10 and -12. Whole-cell lysates from normal keratinocytes (HCK = control cells), oncogenically modified keratinocytes (+E6E7 = LSILs; +Hras = HSILs; +c-Myc = invasive lesions) and 3 cervical cancer cell lines (QG-U, SKG-IIIb and Yumoto) were analyzed using specific antibodies. β-actin served as a loading control. **a**, **b** Immunoblotting of ADAM-9 shows 3 distinctive bands: precursor, mature and processed at 114, 85 and 50 kDa, respectively. **c**, **d** Immunoblotting of ADAM-10 (band at approx. 85 kDa). **e**, **f** Immunoblotting of ADAM-12 protein (band at approx. 84 kDa). The densitometric ratios of the respective ADAM to β-actin are shown in the lower panels. These results are representative of 3 independent experiments. AU = Arbitrary units. * $p < 0.05$.

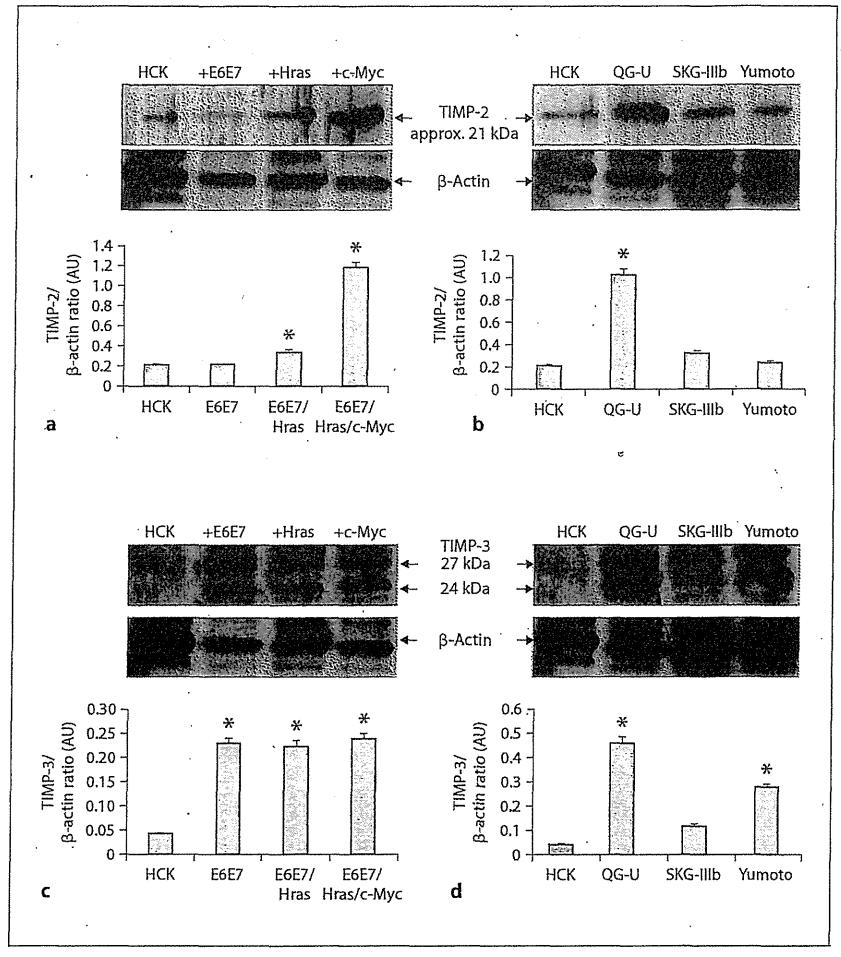

Fig. 4. Immunoblotting of TIMP-2 and TIMP-3. Whole-cell lysates from normal keratinocytes (HCK = control cells), oncogenically modified keratinocytes (+E6E7 = LSILs; +Hras = HSILs; +c-Myc = invasive lesions) and 3 cervical cancer cell lines (QG-U, SKG-IIIb and Yumoto) were analyzed using specific antibodies. β-actin served as a loading control. **a**, **b** Immunoblotting of TIMP-2 protein (band at 21 kDa). **c**, **d** Immunoblotting of TIMP-3 showed bands at 27 and 24 kDa, which represent the glycosylated and nonglycosylated forms, respectively. The densitometric ratios of the respective TIMP to β-actin are shown in the lower panels. These results are representative of 3 independent experiments. AU = Arbitrary units. * $p < 0.05$.

Immunoblotting of TIMP-2 (21 kDa) showed overexpression in E6E7/Hras/c-Myc cells compared to the other cells ($p < 0.05$; fig. 4a). Similarly, the level of TIMP-2 was higher in the QG-U cervical cancer cell line in comparison to the normal keratinocytes ($p < 0.05$; fig. 4b). Expression of TIMP-3 could be detected at 24 and 27 kDa, which represent the nonglycosylated and the glycosylated forms, respectively. Normal keratinocytes showed faint bands at the expected size that become more distinctive and overexpressed in oncogenically modified keratinocytes (fig. 4c). Similarly, cervical cancer cell lines (QG-U and Yumoto) showed upregulated TIMP-3 compared to normal keratinocytes (fig. 4d).

Immunohistochemistry

To verify the in vitro findings, we stained for ADAM-9, ADAM-10 and TIMP-3 using cervical preinvasive and invasive cervical tissues. Immunostaining was able to determine protein localization and distribution.

Immunostaining of ADAM-9

Immunostaining showed that ADAM-9 was weakly expressed in squamous epithelial cells from normal cervical tissues and localized to the superficial epithelial layers with a membranous staining pattern (fig. 5a, b). LSILs showed moderate immunostaining for ADAM-9 that involved the superficial layers in addition to the parabasal layers (fig. 5c, d). Strong immunoreactivity was noticed in most HSILs, with intense staining confined to the basal layer. In HSILs, both cytoplasmic and membranous staining was observed (fig. 5e, f). Squamous cell carcinoma revealed intense immunostaining for ADAM-9, with nuclear and cytoplasmic distribution (fig. 5g, h). Statistical tests showed that expression of

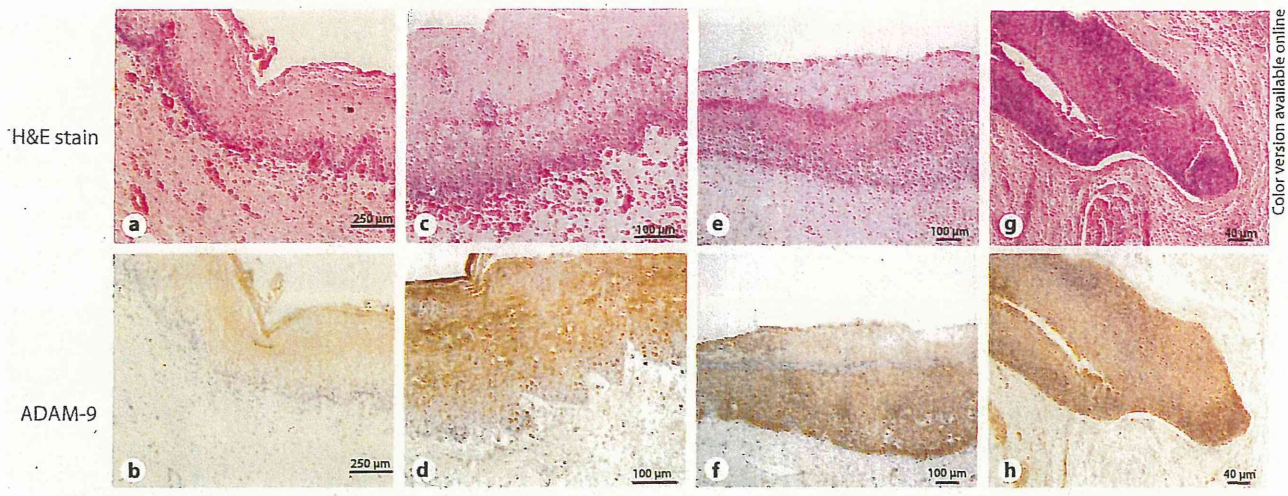

Fig. 5. Immunohistochemistry of ADAM-9 with hematoxylin (H&E) counterstaining. Expression of ADAM-9 increased with increasing severity of dysplasia in cervical squamous epithelia. **a**, **b** ADAM-9 expression is absent or weak in benign cervical epithelia. ×40. **c**, **d** In the LSIL, the expression of ADAM-9 is evident in the superficial layers with some scattering in the basal layer. ×100. **e**, **f** In the HSIL, ADAM-9 immunostaining is present in the full thickness with strong intensity in the basal layer. ×40. **g**, **h** Prominent expression of ADAM-9 is noted in the invasive cancer cells. ×100.

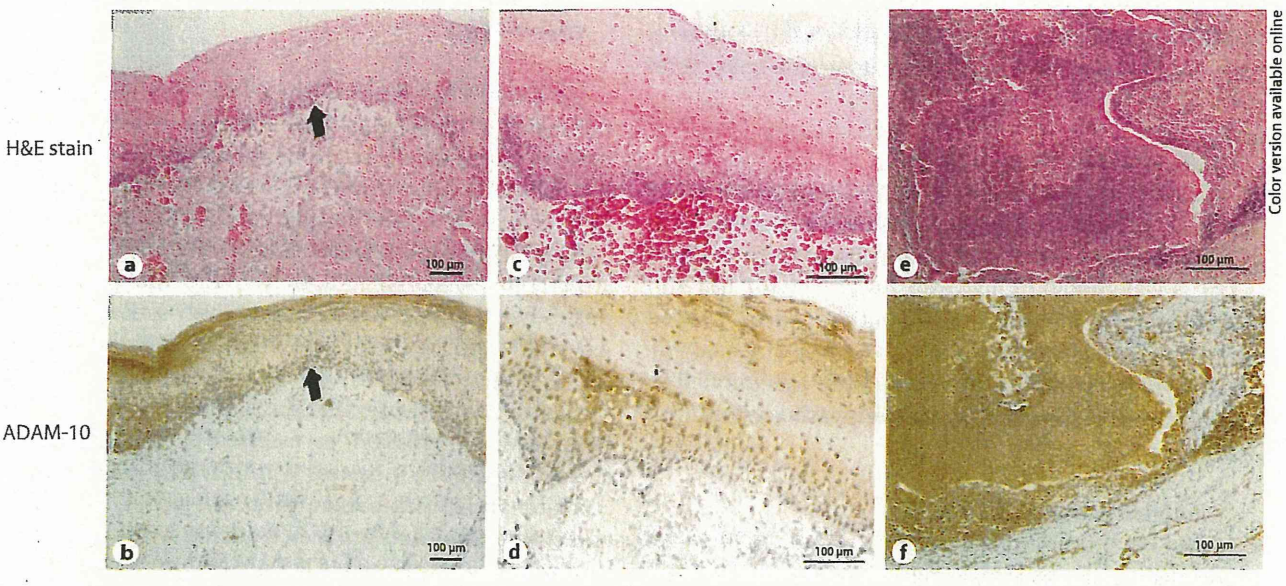

Fig. 6. Immunohistochemical detection of ADAM-10 with hematoxylin (H&E) counterstaining. **a**, **b** Note the transitional zone (arrow) between the normal epithelium (right) and the LSIL (left). ×40. ADAM-10 expression showed increased immunoreactivity as lesions became dysplastic (**b**). **c**, **d** In the LSIL, the expression of ADAM-10 is noticed in the basal and some parabasal layers. ×100. **e**, **f** Strong expression of ADAM-10 is noticed in the cancer nests in invasive cancer. ×100.

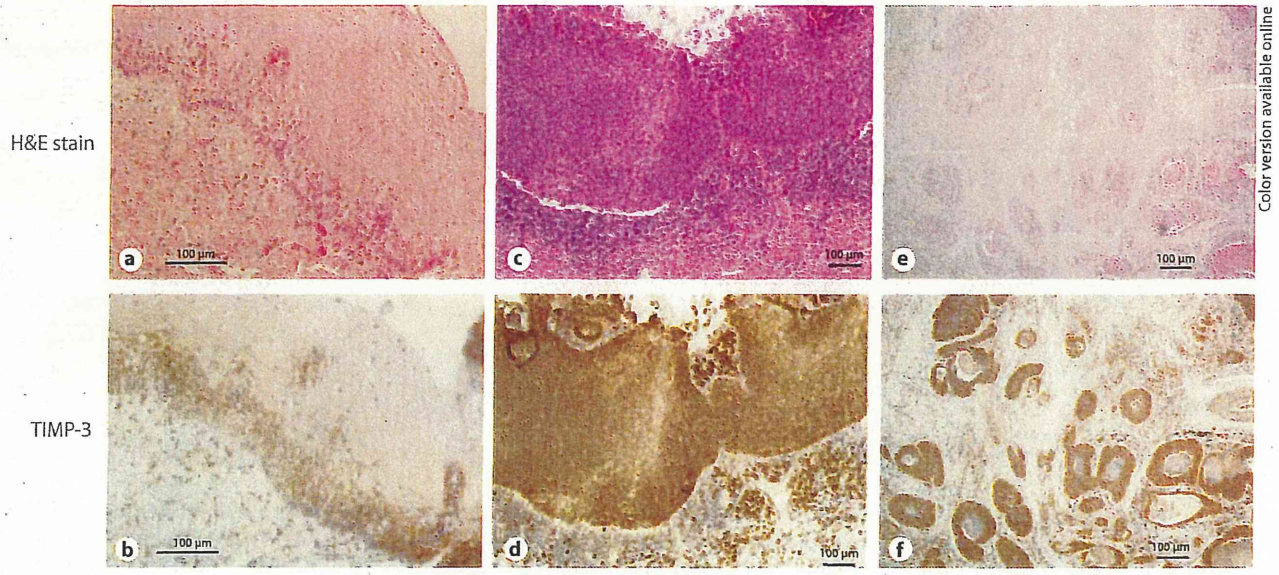

Fig. 7. Immunohistochemistry of TIMP-3 with hematoxylin (H&E) counterstaining. **a**, **b** Weak immunostaining of TIMP-3 is noted in the LSIL. ×100. **c**, **d** TIMP-3 showed moderate staining in the HSIL. ×40. **e**, **f** Strong immunoreactivity of TIMP-3 can be noted in the cancer nests in invasive cancer. ×40.

ADAM-9 is significantly upregulated in HSILs and invasive cancer compared to benign squamous epithelium ($p < 0.05$).

Immunostaining of ADAM-10

Normal cervical tissue showed absent or weak staining for ADAM-10. Dysplastic cells showed reactivity to ADAM-10 antibody (fig. 6a, b). The staining intensity of LSILs was moderate and was mainly in the basal and parabasal layers (fig. 6c, d). Invasive cancer showed strong immunostaining for ADAM-10 (fig. 6e, f). ADAM-10 expression was significantly upregulated in invasive cancer compared to the preinvasive lesions ($p < 0.05$).

Immunostaining of TIMP-3

Scattered immunoreactivity for TIMP-3 could be detected in the normal cervical mucosa. LSILs showed weak immunoreactivity confined to the basal layer (fig. 7a, b). Moderate to strong immunostaining for TIMP-3 was noticed in HSILs (fig. 7c, d), with diffuse strong immunoreactivity in invasive cancer (fig. 7e, f). TIMP-3 staining showed both nuclear and cytoplasmic patterns. Expression of TIMP-3 in squamous cell carcinoma and HSILs was significantly upregulated compared to LSILs and normal epithelium ($p < 0.05$).

Discussion

This study provides novel evidence for dysregulated expression of disintegrin proteins in squamous cell carcinoma of the uterine cervix and its precursor lesions. The mRNA level of ADAM-9, as well as the processed form of ADAM-9 protein (approx. 50 kDa), was found to be significantly upregulated when cells become oncogenically mutated compared to only virally infected cells. It was shown that a processed, alternatively spliced form of ADAM-9 is necessary for invasion through its binding to $\alpha6\beta4$ and $\alpha2\beta1$ integrins of colon cancer cells [30]. This work also demonstrates that the frequency and intensity of ADAM-9 expression, as assessed by immunohistochemical analysis, increases within HSILs and invasive carcinoma relative to LSILs and normal cells. Our immunohistochemical data are in accordance with a previous report indicating increased ADAM-9 immunoreactivity in both cervical intraepithelial neoplasia grade 3 (CIN3) and invasive tumors of the uterine cervix [31]. Physiologically, it was shown that mouse ADAM-9 is not essential for normal development or adult homeostasis [32]. However, human ADAM-9 was found to regulate keratinocyte migration through interaction with $\beta1$ integrins and modulation of MMP synthesis [33]. The expression of ADAM-9 was previously reported to be upregulated at

the mRNA and/or protein level in various solid cancers [34–36]. Furthermore, ADAM-9 overexpression in lung tumor is correlated with brain metastasis [37]. Hence, the biological role of ADAM-9 in cancer could relate to its ability to bind integrins and to degrade extracellular matrix, which promote cell invasion [30]. In addition, blocking ADAM-9 in gastric cancer resulted in inhibition of cell growth of gastric cancer cell lines [38].

Our study describes, for the first time, the expression and regulation of ADAM-10 during cervical carcinogenesis. ADAM-10 was upregulated in oncogenically mutated keratinocytes compared to normal or virally infected cells. The result was confirmed by examining the immunoreactivity of ADAM-10 in preinvasive and invasive cervical tissues. It was found that ADAM-10 could cleave several extracellular matrix components, such as collagen IV of the basement membrane [39], and can also increase the motility of keratinocytes through its ability to shed soluble basement membrane collagen XVII (BPAG2), which supports interactions between the basal cells and the underlying basement membrane [40]. Aberrant expression of collagen XVII in invasive cervical lesions has been investigated elsewhere [41]. However, the relationship between collagen XVII and ADAM-10 in cervical lesions requires further study. Overexpression of ADAM-10 was also found in prostate and oral cancers [42, 43].

This work describes the novel expression of ADAM-12 in cervical carcinogenesis. Interestingly, normal keratinocytes did not express ADAM-12, while virally infected and oncogenically modified keratinocytes showed ADAM-12 expression. As shown by quantitative RT-PCR, the long form of ADAM-12, but not the short form, was only found to be upregulated during cervical carcinogenesis. This finding is similar to the expression of ADAM-12 in lung and bladder cancers [44, 45]. Experimental studies showed that the ADAM-12 level is associated with cancer through degradation of extracellular matrix, as well as regulation of cell proliferation and apoptosis [46, 47]. Earlier studies showed that the cytoplasmic parts of ADAM-12 and ADAM-15 interact with Src homology 3 domain to exert their actions [48, 49].

Taking these findings together, we can conclude that the upregulation of ADAM-12 by invasive cervical cells, compared to absent expression in normal cells, plays an important role in the steps of cervical carcinogenesis.

TIMPs, endogenous regulators of MMPs, can selectively inhibit several ADAMs and ADAMTSs [48]. Therefore, TIMPs can regulate the degradation of extracellular matrix and control cell ligand shedding. Immunoblotting assays showed upregulation of TIMP-2 and TIMP-3 during the course of cervical carcinogenesis, with the highest expression in the invasive phenotype. Biologically, TIMP-2 can selectively inhibit ADAM-12, while TIMP-3 has a wide range of inhibitory effects against ADAMs, including ADAM-10 and ADAM-12 [50, 51].

The expression of TIMPs, in relation to ADAMs, was reported to be dysregulated during several pathological conditions [52]. The aberrant expression of TIMP-2 and -3 in cervical lesions might be biologically relevant, but not exclusively, to the activities of the investigated ADAMs. Based on quantitative RT-PCR results, the selected ADAMTS members might have no role during cervical neoplasia, such as ADAMs do.

In summary, the dysregulated expression of several ADAMs during cervical carcinogenesis can be best noticed when cervical cells acquire genetic alteration(s), as infection with HPV alone, as seen in LSILs, is not enough to provoke ADAM expression significantly. However, synergistic effects of viral oncoproteins and genetic change(s) cannot be ruled out. We can conclude that the expression of several ADAMs, as well as their endogenous regulators, is dysregulated in cervical neoplasia. ADAM-9, -10 and -12 are overexpressed in HSILs and cancerous cells, suggesting that these proteins could play a crucial role in the pathogenesis of cervical carcinoma. The exact mechanism of action requires further studies to determine the biological effects of these proteins during the cascades of cervical neoplasia.

References

1 Thun MJ, DeLancey JO, Center MM, Jemal A, Ward EM: The global burden of cancer: priorities for prevention. Carcinogenesis 2010;31:100–110.

2 Stoler MH: Human papillomaviruses and cervical neoplasia: a model for carcinogenesis. Int J Gynecol Pathol 2000;19:16–28.

3 Münger K, Baldwin A, Edwards KM, Hayakawa H, Nguyen CL, Owens M, Grace M, Huh K: Mechanisms of human papillomavirus-induced oncogenesis. J Virol 2004;78:11451–11460.

4 zur Hausen H: Papillomaviruses and cancer: from basic studies to clinical application. Nat Rev Cancer 2002;2:342–350.

5 Wolfsberg TG, Primakoff P, Myles DG, White JM: ADAM, a novel family of membrane proteins containing A Disintegrin And Metalloprotease domain: multipotential functions in cell-cell and cell-matrix interactions. J Cell Biol 1995;131:275–278.

6 Jones GC, Riley GP: ADAMTS proteinases: a multi-domain, multi-functional family with roles in extracellular matrix turnover and arthritis. Arthritis Res Ther 2005;7:160–169.
7 Van Goor H, Melenhorst WB, Turner AJ, Holgate ST: Adamalysins in biology and disease. J Pathol 2009;219:277–286.
8 Higuchi Y, Yasui A, Matsuura K, Yamamoto S: CD156 transgenic mice. Different responses between inflammatory types. Pathobiology 2002;70:47–54.
9 Shiomi T, Lemaître V, D'Armiento J, Okada Y: Matrix metalloproteinases, a disintegrin and metalloproteinases, and a disintegrin and metalloproteinases with thrombospondin motifs in non-neoplastic diseases. Pathol Int 2010;60:477–496.
10 Eto K, Huet C, Tarui T, Kupriyanov S, Liu HZ, Puzon-McLaughlin W, Zhang XP, Sheppard D, Engvall E, Takada Y: Functional classification of ADAMs based on a conserved motif for binding to integrin alpha 9 beta1: implications for sperm-egg binding and other cell interactions. J Biol Chem 2002; 277:17804–17810.
11 Yang P, Baker KA, Hagg T: The ADAMs family: coordinators of nervous system development, plasticity and repair. Prog Neurobiol 2006;79:73–94.
12 Gilpin BJ, Loechel F, Mattei MG, Engvall E, Albrechtsen R, Wewer UM: A novel, secreted form of human ADAM 12 (meltrin alpha) provokes myogenesis in vivo. J Biol Chem 1998;273:157–166.
13 Kawaguchi N, Xu X, Tajima R, Kronqvist P, Sundberg C, Loechel F, Albrechtsen R, Wewer UM: ADAM 12 protease induces adipogenesis in transgenic mice. Am J Pathol 2002;160:1895–1903.
14 Duffy MJ, McKiernan E, O'Donovan N, McGowan PM: Role of ADAMs in cancer formation and progression. Clin Cancer Res 2009;15:1140–1144.
15 Mochizuki S, Okada Y: ADAMs in cancer cell proliferation and progression. Cancer Sci 2007;98:621–628.
16 Apte SS: A disintegrin-like and metalloprotease (reprolysin-type) with thrombospondin type 1 motif (ADAMTS) superfamily: functions and mechanisms. J Biol Chem 2009;284:31493–31497.
17 Liu YJ, Xu Y, Yu Q: Full-length ADAMTS-1 and the ADAMTS-1 fragments display pro- and antimetastatic activity, respectively. Oncogene 2006;25:2452–2467.
18 Rocks N, Paulissen G, El Hour M, Quesada F, Crahay C, Gueders M, Foidart JM, Noel A, Cataldo D: Emerging roles of ADAM and ADAMTS metalloproteinases in cancer. Biochimie 2008;90:369–379.
19 Murphy G: The ADAMs: signalling scissors in the tumour microenvironment. Nat Rev Cancer 2008;8:929–941.
20 Maskos K, Fernandez-Catalan C, Huber R, Bourenkov GP, Bartunik H, Ellestad GA, Reddy P, Wolfson MF, Rauch CT, Castner BJ, Davis R, Clarke HR, Petersen M, Fitzner JN, Cerretti DP, March CJ, Paxton RJ, Black RA, Bode W: Crystal structure of the catalytic domain of human tumor necrosis factor-alpha-converting enzyme. Proc Natl Acad Sci USA 1998;95:3408–3412.
21 Brew K, Dinakarpandian D, Nagase H: Tissue inhibitors of metalloproteinases: evolution, structure and function. Biochim Biophys Acta 2000;1477:267–283.
22 Amour A, Knight CG, Webster A, Slocombe PM, Stephens PE, Knäuper V, Docherty AJ, Murphy G: The in vitro activity of ADAM-10 is inhibited by TIMP-1 and TIMP-3. FEBS Lett 2000;473:275–279.
23 Kashiwagi M, Tortorella M, Nagase H, Brew K: TIMP-3 is a potent inhibitor of aggrecanase 1 (ADAM-TS4) and aggrecanase 2 (ADAM-TS5). J Biol Chem 2001;276:12501–12504.
24 Hanahan D, Weinberg RA: The hallmarks of cancer. Cell 2000;100:57–70.
25 Sheu BC, Lien HC, Ho HN, Lin HH, Chow SN, Huang SC, Hsu SM: Increased expression and activation of gelatinolytic matrix metalloproteinases is associated with the progression and recurrence of human cervical cancer. Cancer Res 2003;63:6537–6542.
26 Libra M, Scalisi A, Vella N, Clementi S, Sorio R, Stivala F, Spandidos DA, Mazzarino C: Uterine cervical carcinoma: role of matrix metalloproteinases. Int J Oncol 2009;34: 897–903.
27 Ueda M, Terai Y, Yamashita Y, Kumagai K, Ueki K, Yamaguchi H, Akise D, Hung YC, Ueki M: Correlation between vascular endothelial growth factor-C expression and invasion phenotype in cervical carcinomas. Int J Cancer 2002;98:335–343.
28 Mitsuhashi A, Tanaka H, Tanaka N, Sugita M, Shirasawa H, Tokita H, Eda H, Sekiya S: Establishment and characterization of a new HPV-negative squamous cell carcinoma cell line (Yumoto) from the human uterine cervix. Gynecol Oncol 1998;70:339–347.
29 Narisawa-Saito M, Yoshimatsu Y, Ohno S, Yugawa T, Egawa N, Fujita M, Hirohashi S, Kiyono T: An in vitro multistep carcinogenesis model for human cervical cancer. Cancer Res 2008;68:5699–5705.
30 Mazzocca A, Coppari R, De Franco R, Cho JY, Libermann TA, Pinzani M, Toker A: A secreted form of ADAM9 promotes carcinoma invasion through tumor-stromal interactions. Cancer Res 2005;65:4728–4738.
31 Zubel A, Flechtenmacher C, Edler L, Alonso A: Expression of ADAM9 in CIN3 lesions and squamous cell carcinomas of the cervix. Gynecol Oncol 2009;114:332–336.
32 Weskamp G, Cai H, Brodie TA, Higashyama S, Manova K, Ludwig T, Blobel CP: Mice lacking the metalloprotease-disintegrin MDC9 (ADAM9) have no evident major abnormalities during development or adult life. Mol Cell Biol 2002;22:1537–1544.
33 Zigrino P, Steiger J, Fox JW, Löffek S, Schild A, Nischt R, Mauch C: Role of ADAM-9 disintegrin-cysteine-rich domains in human keratinocyte migration. J Biol Chem 2007; 282:30785–30793.
34 O'Shea C, McKie N, Buggy Y, Duggan C, Hill AD, McDermott E, O'Higgins N, Duffy MJ: Expression of ADAM-9 mRNA and protein in human breast cancer. Int J Cancer 2003; 105:754–761.
35 Zigrino P, Mauch C, Fox JW, Nischt R: Adam-9 expression and regulation in human skin melanoma and melanoma cell lines. Int J Cancer 2005;116:853–859.
36 Peduto L, Reuter VE, Shaffer DR, Scher HI, Blobel CP: Critical function for ADAM9 in mouse prostate cancer. Cancer Res 2005;65: 9312–9319.
37 Shintani Y, Higashiyama S, Ohta M, Hirabayashi H, Yamamoto S, Yoshimasu T, Matsuda H, Matsuura N: Overexpression of ADAM9 in non-small cell lung cancer correlates with brain metastasis. Cancer Res 2004;64:4190–4196.
38 Carl-McGrath S, Lendeckel U, Ebert M, Roessner A, Rocken C: The disintegrin-metalloproteinases ADAM9, ADAM12, and ADAM15 are upregulated in gastric cancer. Int J Oncol 2005;26:17–24.
39 Millichip M, Dallas D, Wu E, Dale S, McKie N: The metallo-disintegrin ADAM10 (MADM) from bovine kidney has type IV collagenase activity in vitro. Biochem Biophys Res Commun 1998;245:594–598.
40 Franzke CW, Tasanen K, Schacke H, Zhou Z, Tryggvason K, Mauch C, Zigrino P, Sunnarborg S, Lee DC, Fahrenholz F, Bruckner-Tuderman L: Transmembrane collagen XVII, an epithelial adhesion protein, is shed from the cell surface by ADAMs. EMBO J 2002;21: 5026–5035.
41 Yamada T, Endo R, Tsukagoshi K, Fujita S, Honda K, Kinoshita M, Hasebe T, Hirohashi S: Aberrant expression of a hemidesmosomal protein, bullous pemphigoid antigen 2, in human squamous cell carcinoma. Lab Invest 1996;75:589–600.
42 McCulloch DR, Akl P, Samaratunga H, Herington AC, Odorico DM: Expression of the disintegrin metalloprotease, ADAM-10, in prostate cancer and its regulation by dihydrotestosterone, insulin-like growth factor I, and epidermal growth factor in the prostate cancer cell model LNCaP. Clin Cancer Res 2004;10:314–323.
43 Ko SY, Lin SC, Wong YK, Liu CJ, Chang KW, Liu TY: Increase of disintergin metalloprotease 10 (ADAM10) expression in oral squamous cell carcinoma. Cancer Lett 2007;245: 33–43.

44 Rocks N, Paulissen G, Quesada Calvo F, Polette M, Gueders M, Munaut C, Foidart JM, Noel A, Birembaut P, Cataldo D: Expression of a disintegrin and metalloprotease (ADAM and ADAMTS) enzymes in human non-small-cell lung carcinomas (NSCLC). Br J Cancer 2006;94:724–730.
45 Fröhlich C, Albrechtsen R, Dyrskjøt L, Rudkjaer L, Ørntoft TF, Wewer UM: Molecular profiling of ADAM12 in human bladder cancer. Clin Cancer Res 2006;12:7359–7368.
46 Roy R, Wewer UM, Zurakowski D, Pories SE, Moses MA: ADAM 12 cleaves extracellular matrix proteins and correlates with cancer status and stage. J Biol Chem 2004;279:51323–51330.
47 Rocks N, Estrella C, Paulissen G, Quesada-Calvo F, Gilles C, Guéders MM, Crahay C, Foidart JM, Gosset P, Noel A, Cataldo DD: The metalloproteinase ADAM-12 regulates bronchial epithelial cell proliferation and apoptosis. Cell Prolif 2008;41:988–1001.
48 Mori S, Tanaka M, Nanba D, Nishiwaki E, Ishiguro H, Higashiyama S, Matsuura N: PACSIN3 binds ADAM12/meltrin alpha and up-regulates ectodomain shedding of heparin-binding epidermal growth factor-like growth factor. J Biol Chem 2003;278:46029–46034.
49 Yasui A, Matsuura K, Shimizu E, Hijiya N, Higuchi Y, Yamamoto S: Expression of splice variants of the human ADAM15 gene and strong interaction between the cytoplasmic domain of one variant and Src family proteins Lck and Hck. Pathobiology 2004;71:185–192.
50 Edwards DR, Handsley MM, Pennington CJ: The ADAM metalloproteinases. Mol Aspects Med 2008;29:258–289.
51 Kveiborg M, Jacobsen J, Lee MH, Nagase H, Wewer UM, Murphy G: Selective inhibition of ADAM12 catalytic activity through engineering of tissue inhibitor of metalloproteinase 2 (TIMP-2). Biochem J 2010;430:79–86.
52 Fedak PW, Moravec CS, McCarthy PM, Altamentova SM, Wong AP, Skrtic M, Verma S, Weisel RD, Li RK: Altered expression of disintegrin metalloproteinases and their inhibitor in human dilated cardiomyopathy. Circulation 2006;113:238–245.